physica status solidi a
www.pss-a.com

Electronic Properties of Bulk and Monolayer TMDs: Theoretical Study Within DFT Framework (GVJ-2e Method)

Julia Gusakova, Xingli Wang, Li Lynn Shiau, Anna Krivosheeva, Victor Shaposhnikov, Victor Borisenko, Vasilii Gusakov, and Beng Kang Tay**

Accurate prediction of band gap for new emerging materials is highly desirable for the exploration of potential applications. The band gaps of bulk and monolayer TMDs (MoS_2, $MoSe_2$, WS_2, and WSe_2) are calculated with the recently proposed by us GVJ-2e method, which is implemented within DFT framework without adjustable parameters and is based on the total energies only. The calculated band gaps are in very good agreement with experimental ones for both bulk and monolayer TMDs. For monolayer MoS_2, $MoSe_2$, WS_2, and WSe_2, direct band gaps are predicted to be 1.88 eV, 1.57 eV, 2.03 eV, 1.67 eV correspondingly, and for bulk TMDs, indirect band gaps of 1.23 eV (MoS_2), 1.09 eV ($MoSe_2$), 1.32 eV (WS_2), 1.21 eV (WSe_2) are predicted. The GVJ-2e method demonstrates good accuracy with mean absolute error (MAE) of about 0.03 eV for TMDs PL gaps (and 0.06 eV for QP gaps). GVJ-2e method allows to equally accurately obtain band gaps for 3D and 2D materials. The errors of GVJ-2e method are significantly smaller than errors of other widely used methods such as GW (MAE 0.23 eV), hybrid functional HSE (MAE 0.17 eV), TB-mBJ functional (MAE 0.14 eV).

1. Introduction

Transition metal dichalcogenides (MX2, M stands for transition metal and X stands for chalcogen) are layered materials, which possess strong bonding in-plane and weak bonding between planes (van der Waals).[1] The first exploration of bulk transition metal dichalcogenides (TMDs) was done decades ago.[1,2] In the recent decades monolayers of TMDs,[3–7] as one kind of the representatives of two dimensional (2D) materials, have attracted much attention owing to their rich physics and promising applications in nanoelectronics and photonics.[8–12]

Significant amount of effort has been devoted to the synthesis of TMD materials and as well to the exploration of their properties.[52–64] Electronic properties of these materials are of a great importance when it comes to applications. In general, the variation of electronic properties of TMDs is determined by the variation of the band structure with the transitions from bulk to monolayer.[13]

Density functional theory (DFT)[14] is a method of choice for theoretical exploration of solids. The approximation of the exchange-correlation energy plays a key role in DFT computations. So, various approximations of the exchange-correlation energy have been developed starting with local density approximation (LDA) and generalized gradient approximation (GGA),[15–17] which allow accurate prediction of many ground state properties including structural properties and stability. Unfortunately, the same is not always true for the electronic properties, where the lack of correlation between experimental and theoretical results could be found as the band gap could be significantly underestimated, and errors can reach even 40%.[18] The latter essentially complicates the theoretical search for new materials with desired electronic properties.

In order to improve the efficiency and accuracy of theoretically obtained electronic properties, hybrid functionals (HSE,[19–21] PBE0,[22] B3LYP[23,24]) and screened exchange (sX) hybrid functionals[25] have been developed. As another attempt to improve the prediction of electronic properties by DFT, LDA + U has been developed in which physics of Hubbard model was incorporated into density functionals.[26–28] Also, the modified version of Becke-Johnson exchange potential[29] has been developed by Tran and Blaha,[30] which contains adjustable parameters. On the other hand, theoretically sophisticated way to solve the band gap problem was suggested by Green's function based methods as in GW approach.[31,32] Nevertheless, although quite often GW (or G0W0) becomes the method of choice, it is known to be quite computationally expensive method, as is the use of hybrid functionals in DFT.

J. Gusakova, L. L. Shiau, Prof. B. K. Tay
Novitas Center, Nanyang Technological University, 50 Nanyang Avenue, 639798 Singapore, Singapore
E-mail: julia001@e.ntu.edu.sg; ebktay@ntu.edu.sg
Dr. X. Wang, Prof. B. K. Tay
CINTRA UMI CNRS/NTU/THALES, 50 Nanyang Drive, 637553 Singapore, Singapore
Dr. A. Krivosheeva, Dr. V. Shaposhnikov, Prof. V. Borisenko
Belarusian State University of Informatics and Radioelectronics, 6 P. Browka, 220013 Minsk, Belarus
Dr. V. Gusakov
Scientific-Practical Materials Research Center of NAS of Belarus, 19 P. Brovki, 220072 Minsk, Belarus

DOI: 10.1002/pssa.201700218

Along with experimental exploration of the TMDs, theoretical investigation of TMDs has been performed to contribute to the search for new materials with desirable electronic properties. The use of LDA for TMD monolayers leads to band gap values underestimated for about 30%.[33] Similarly PBE[34] GGA and GGA + U underestimate band gap for about 30%,[13,35–38] while B3LYP overcorrects band gap values for about 0.7 eV.[36] It has been shown that for bulk TMDs PBE performs better than hybrid PBE0, the latter of which tends to overestimate the band gap for about 1 eV.[36] When HSE hybrid functional was used, band gaps for both bulk and monolayer TMDs were overestimated for about 0.2 eV.[36,39] Very similar performance has been shown with the use of screened exchange functional (sX).[40] GW (or G_0W_0) is also used to compute electronic properties and band gaps of TMD. Although GW produces satisfactory results for bulk forms,[35,41,42] it usually significantly overestimates band gaps for monolayers for about 0.5–0.7 eV.[33,43] The large errors make it difficult to predict the electronic properties of new materials precisely with current calculation methods.

It should also be noted that methods and approximations, which perform well on bulk TMDs, will not necessarily demonstrate good performance on monolayer TMDs. Thus, method which will perform equally well in estimation of the band gap of both bulk (3D) and monolayer (2D) TMDs is needed.

Recently, a new general method (GVJ-2e) was proposed by us for band gap computation within DFT framework,[44] which is based solely on the total energy computations and is adjustable parameter free. The method has been verified on a set of traditional bulk semiconductors (Si, C, etc.) and wide gap insulators (Xe, Kr), and the calculated band gap values were obtained almost with experimental accuracy.[45]

In this paper, we present detailed analysis of the theoretical band gap of both bulk and monolayer TMDs (MoS_2, $MoSe_2$, WS_2, and WSe_2) calculated with GVJ-2e method.[45] We extend the application of GVJ-2e method beyond traditional 3D materials to the band gap calculations of bulk TMDs and monolayer TMDs as one of representatives of 2D materials and analyze the theoretical GVJ-2e band gap in comparison with the experimental data collected from the reported references and our own PL measurements. In addition, we compare the accuracy of GVJ-2e method with other well-accepted theoretical methods.

2. Theoretical Background

The fundamental band gap is defined as the difference between the ionization potential and electron affinity[46,49] which are determined when one particle is added or removed from a solid:

$$E_g \equiv I - A = E^{(0)}_{N+1} + E^{(0)}_{N-1} - 2E^{(0)}_N, \tag{1}$$

where $E^{(0)}_{N+1}, E^{(0)}_{N-1}, E^{(0)}_N$ are the ground state total energy functionals of the system with $N+1$, N–1, and N electrons. The total energy functional is traditionally represented as a sum of the kinetic energy functional, Hartree functional, the functional representing interaction with external field, and the exchange-correlation energy functional. In order to compute a band gap through Eq. (1), one should select an approximation for the exchange-correlation energy functional, the analytical expression of which is not available. The local density approximation (LDA)[15] is one of the most widely used, and it has demonstrated satisfactory results for the ground state properties of solids. However, when electronic properties, and especially the band gap, are considered, results do not always correlate with the experiment. Germanium is an example, where computation of the band gap with LDA approximation for the exchange-correlation energy fails, as the calculated band gap turns out to be about 0 eV.[45]

In the previous work,[45] we have determined the fundamental band gap through the ground state total energies of a system when pair of electrons is removed from HOMO orbital (ionization) and added to LUMO orbital (electron affinity):

$$E_g = 0.5\left(E^{(0)}_{N+2} + E^{(0)}_{N-2} - 2E^{(0)}_N\right), \tag{2}$$

where $E^{(0)}_{N+2}, E^{(0)}_{N-2}, E^{(0)}_N$ are the ground state total energy functionals of the system with N + 2, N–2, and N electrons (two charged systems with total charge Z = –2, Z = +2 and a neutral system with Z = 0 respectively). It is important to note that the Eq. (2) is more accurate in LDA approximation in comparison with the traditionally used Eq. (1).[45]

In GVJ-2e method, we have derived a final nonlinear equation for the band gap based only on the total energy functionals of density. In order to obtain the final nonlinear equation of the band gap we considered two ensembles. The first ensemble consisted of two identical neutral systems of solid. The second ensemble contained two charged systems; one system had the total charge +2, and the other had the total charge −2. The systems in these ensembles did not interact with each other. Also, in order to obtain the final equation within derivation, we decomposed the exact exchange-correlation energy functional in two terms: a local part of exchange-correlation energy (which could be calculated in LDA) and a nonlocal part of exchange-correlation energy. The insight on the derivation could be found in the paper.[45]

The final nonlinear equation for the fundamental band gap includes LDA band gap and two correction terms taking into account nonlocal part of the exchange correlation energy functional and has the form:

$$E^{(0)}_g = E^{(\mathrm{LDA})}_g + \frac{1}{2}\Delta^{\infty}_{XC} - \frac{1}{2}E^{(\infty,\mathrm{xc})}_{(1,0)}\left(1 + \exp\left(-\frac{E^{(0)}_g}{E_0}\right)\right), \tag{3}$$

where $E^{(0)}_g$ is the band gap, E_0 is used for the dimensionless energy in the exponent (in the following calculations is taken equal E_0 = 1 eV). The $E^{(\mathrm{LDA})}_g$ is the band gap calculated according to the Eq. (2), where the total energies for neutral and charged systems are calculated in LDA approximation (LDA2e). Δ^{∞}_{XC} and $E^{(\infty,\mathrm{xc})}_{(1,0)}$ are the correction terms and their precision defines the precision of the band gap value calculation. These correction terms could be obtained from the following equations:

$$\Delta^{\infty}_{XC} = \left(E_{\mathrm{ens.2}} - E_{\mathrm{ens.1}}\right)^{(0)} - \left(E_{\mathrm{ens.2}} - E_{\mathrm{ens.1}}\right)^{(\mathrm{LDA})}, \tag{4}$$

$$E_{(1,0)}^{(\infty,\mathrm{xc})} = \left(E_{Z=0}^{(0)} - E_{Z=0}^{(\mathrm{LDA})}\right) - \left(E_{Z=+2}^{(0)} - E_{Z=+2}^{(\mathrm{LDA})}\right), \quad (5)$$

where the total energies of ensembles are equal to $E_{\mathrm{ens.2}} = E_{Z=+2} + E_{Z=-2}$ and $E_{\mathrm{ens.1}} = 2E_{Z=0}$ correspondingly. The correction term $E_{(1,0)}^{(\infty,\mathrm{xc})}$ describes a nonlocal part of the exchange-correlation interaction of the pair of electrons at HOMO with the rest of the neutral system. In Eqs. (3), (4), and (5), all the quantities included are the total energies of neutral ($Z=0$) and charged systems ($Z=+2$ and $Z=-2$).

The final form of the Eq. (3) has been obtained with the assumption for the limit of nonlocal part of the exchange-correlation energy between the two outer pairs of electrons of system with N + 2 electrons: $\lim_{Eg\to 0} E_{(12,\mathrm{Eg})}^{(\infty,\mathrm{xc})} = E_{(12,0)}^{(\infty,\mathrm{xc})} \approx E_{(1,0)}^{(\infty,\mathrm{xc})}$. The term $E_{(12,\mathrm{Eg})}^{(\infty,\mathrm{xc})}$ describes a nonlocal part of the exchange-correlation energy between (1) and (2) pairs of electrons in the system with N + 2 electrons. It has been demonstrated[45] that such approximation gives good results for band gap computation for such 3D materials as C, Si, Ge, LiF, BN and as well for wide gap insulators (Xe, Kr). In general case, the limit of $E_{(12,\mathrm{Eg})}^{(\infty,\mathrm{xc})}$ when $E_g \to 0$ depends on the orbitals to which electron pairs (1) and (2) belong. In the case of TMDs, pair (1) belongs to d orbital (molybdenum) or to f orbital (tungsten) which are more delocalized comparing to s and p orbitals. Thus, we have used the following approximation of the limit $\lim_{Eg\to 0} E_{(12,\mathrm{Eg})}^{(\infty,\mathrm{xc})} = E_{(12,0)}^{(\infty,\mathrm{xc})} \approx E_{(1,0)}^{(\infty,\mathrm{xc})} - E_{(2,0)}^{(\infty,\mathrm{xc})}$ for TMD materials. It should be emphasized that the accuracy of the band gap calculation is determined by the accuracy of calculation Δ_{XC}^{∞} and $E_{(1,0)}^{(\infty,\mathrm{xc})}$, while the last is determined by the approximation used for the exchange-correlation energy and used pseudopotentials. There are two approaches for calculating correction terms, the one is a molecular cluster method without using the pseudopotentials, and the other is a crystal supercell method. In this study, all calculations are made within the framework of a supercell method.

3. Experiment Materials

MoO_3 powder (99.5%), WO_3 powder (99.9%), S powder (99.5%), Se powder (99.9%).

3.1. Growth of Monolayers

In this work, besides the experimental data collected from reported references, MoS_2, $MoSe_2$, WS_2, and WSe_2 monolayers were also grown to determine their direct gaps. All the TMDs were grown with chemical vapor deposition, which have been widely used for the growth of TMD monolayers with high quality.[46–48] MoO_3 and WO_3 powders were used as precursors of molybdenum dichalcogenides (MoX_2, X stands for S and Se) and tungsten dichalcogenides (WX_2) respectively. Sulfur and selenium powders were used for the growth of sulfides and selenides respectively. For the growth, the oxides with a piece of SiO_2 wafer suspended were heated up to the reaction temperature (800 °C for MoX_2, while 900 °C for WX_2), while the chalcogen powders were heated to their melting points. The heating rate was 50 °C min^{-1}. After reaching the reaction temperature, the system was kept at this temperature for 15 min for the material growth. Then system was cooled down to room temperature naturally. Ar was used as carrier gas to carry the chalcogen vapor into the high temperature region with 60 sccm flow rate. It should be noted that for the growth of selenides 10 sccm H_2 was also required to assist the reduction of the oxides during the reaction.[47,48]

3.2. Characterization

After CVD growth, the direct band gap of each monolayer was characterized and the photoluminescence (PL) spectra were collected with a WITEC alpha 300R system. A diode laser of 532 nm was used as an excitation light source. The power of the laser was less than 1 mW to avoid the thermal effect. Optical images of monolayers and PL spectra after Lorentz fitting are presented on the Figure S1 in supporting information. The peaks were located at 1.87 eV (MoS_2), 1.52 eV ($MoSe_2$), 1.99 eV (WS_2), and 1.62 eV (WSe_2).

4. Results and Discussion

We have considered following semiconducting TMDs: MoS_2, $MoSe_2$, WS_2, WSe_2, all of which possessing the hexagonal symmetry with the space group $P6_3/mmc$. The TMD monolayer (1L) contains three atomic planes in the configuration when two chalcogen (S or Se) planes sandwich the plane of metal atoms (Mo or W). Bulk TMD is formed when monolayers are stacked together with weak inter-plane but strong intra-plane interactions.

Quantum Espresso implementation of the DFT was used for the computation of structural and electronic properties of bulk and monolayer TMDs. We used PZ LDA[15] and PBE GGA[34] approximations of the exchange-correlation energy and pseudopotentials. Brillouin zone was sampled using Monkhorst-Pack approach, $12 \times 12 \times 3$ and $10 \times 10 \times 1$ meshes were used for the bulk and monolayer correspondingly. The kinetic energy cutoff was set to 40 Ry (MoS_2 and $MoSe_2$) and 50 Ry (WS_2 and WSe_2).

First, we performed the lattice relaxation computation for all bulk materials under consideration in order to obtain optimum lattice parameters. The calculated values of the relaxed lattice parameters and experimental ones are presented in **Table 1**. The deviation of the relaxed lattice parameters a and c for both PZ LDA and PBE GGA is mostly within 1% when compared to the experimental ones. In all subsequent computations, the relaxed lattice parameters were used.

For the bulk and monolayer TMDs (MoS_2, $MoSe_2$, WS_2, WSe_2) the band gaps were computed using GVJ-2e method according to the Eq. (3). With the GVJ-2e approach first we obtained the quasi-particle (QP) gap, from which PL band gap (E_g^{PL}) has been calculated using equation $E_g^{\mathrm{PL}} = E_g^{\mathrm{QP}} - E_{\mathrm{exc.binding}}$. In the present work the values of the exciton binding energies ($E_{\mathrm{exc.binding}}$) were obtained from the

Table 1. Relaxed lattice parameters for bulk MoS_2, $MoSe_2$, WS_2, WSe_2, and experimental lattice parameters. All lattice parameters are given in Å.

	MoS_2	$MoSe_2$	WS_2	WSe_2
PZ LDA				
a	3.139	3.276	3.136	3.261
c	12.182	12.948	12.375	13.005
PBE GGA				
a	3.194	3.338	3.194	3.312
c	12.435	12.983	12.640	13.199
Experiment				
a	3.160	3.288	3.153	3.280
c	12.295	12.900	12.323	12.950
Ref.	[50]	[50]	[51]	[50]

Bethe-Salpeter equation (BSE),[65] as there exists variability in the experimental values for exciton binding energies in monolayer TMDs. The results for GVJ-2e QP gap and GVJ-2e optical band gap (GVJ-2e PL) are provided in Tables 2 and 3. In the **Table 2** we present comparison of the theoretically obtained values for GVJ-2e QP gap with the experimentally obtained QP gap from the scanning tunnelling spectroscopy (STS). Here we also give values for GW and G_0W_0 band gaps which are compared with STS QP gap values.

From the Table 2 follows that GVJ-2e QP gaps of TMD monolayers are in good agreement with STS QP experimentally obtained values having mean absolute error (MAE) of about 0.10 eV and mean absolute percentage deviation (MAPD) of 4%. Comparison of QP gaps with experimental STS data for TMD monolayers for GW yields MAE of 0.42 eV (MAPD 18%) and for G_0W_0 method MAE is about 0.09 eV (MAPD 3%).

In the **Table 3** both QP and PL band gaps obtained with GVJ-2e method are provided. As it follows from the Tables 2 and 3, the GVJ-2e method allows obtaining the band gap values correlating well with the experimentally obtained band gap for both bulk and monolayer TMDs. For bulk and monolayer TMDs, the GVJ-2e method demonstrates MAE of 0.03 eV and MAPD of about 2% for optical gap evaluation; for the GVJ-2e QP gap MAE is of 0.06 eV (MAPD 2%). The comparison of the theoretical and experimental PL band gap values is demonstrated in the **Figure 1**. The theoretical set of band gaps includes values calculated with our GVJ-2e method and well-accepted HSE, TB-mBJ, sX methods.

Table 2. TMD monolayers QP gaps: theoretical – obtained from GW and G_0W_0; calculated with GVJ-2e method (Eq. (3)); experimental – obtained from STS measurement. BSE are the theoretical exciton binding energies in TMD 1L. All values are in eV.

1L	G_0W_0 & GW	Exciton BSE	GVJ-2e QP	Exp.
MoS_2	2.48[a]	0.501[c]	2.38	2.40[d]
	2.97[b]			2.5[e]
$MoSe_2$	2.18[a]	0.465[c]	2.03	2.18[f]
	2.41[b]			
WS_2	2.43[a]	0.481[c]	2.51	2.73[g]
WSe_2	2.08[a]	0.442[c]	2.11	2.12[h]

[a] G0W0 Ref. [33]; [b] GW Ref. [41]; [c] BSE Ref. [65]; [d] Ref. [59]; [e] Ref. [66]; [f] Ref. [67]; [g] Ref. [68]; [h] Ref. [69].

There exists variability in the published experimental values (including our own values from the PL measurement) for the band gap of monolayers of TMDs (as listed in Table 3).[52–64] The experimentally obtained band gaps are 1.87–1.92 eV (MoS_2), 1.55–1.58 eV ($MoSe_2$), 1.98–2.05 eV (WS_2), 1.6–1.66 eV (WSe_2).[52–64] It should be noted that PL band gaps obtained theoretically with our GVJ-2e method are 1.88 eV (MoS_2), 1.57 eV ($MoSe_2$), 2.03 eV (WS_2), 1.67 eV (WSe_2), which correlate well with both our experimental results and the experimental results published by other groups.

In order to compute the band gap according to the Eq. (3), one first needs to compute the LDA band gap. It is important to underline that the equation for LDA_{2e} (Eq. (2)) should be used. Equation (2) produces LDA_{2e} band gap, which usually has better correlation with experiment than LDA band gaps obtained with Eq. (1).[45] Calculated LDA_{2e} band gap values for bulk and monolayer TMDs are presented in Table 3. For monolayers, the following values are available from the literature for the LDA band gap: 1.58 eV (MoS_2), 1.32 ($MoSe_2$), 1.51 eV (WS_2), and 1.22 eV (WSe_2).[33] Thus the mean absolute error for TMD monolayer of LDA band gap is 0.37 eV, while for LDA_{2e} this error is about 0.32 eV (compare with LDA_{2e} mean absolute error for bulk TMDs of 0.10 eV).

The comparison of the band gap calculated with GVJ-2e and LDA_{2e} methods reveals that taking account of nonlocal part of the exchange-correlation energy plays a crucial role for precision of band gap calculation. The latter is implemented by means of including correction terms. Quite often, the correction terms have magnitudes, which are comparable with magnitudes of the band gap.

The correction term $E_{(1,0)}^{(\infty,xc)}$ represents a nonlocal part of the exchange-correlation energy of pair of electrons on HOMO of a neutral system with the rest of the system. There is a significant difference in HOMO of MoX_2 and WX_2 systems, where d and f orbitals correspond to the first and the second case (X is either S or Se). Thus, for MoX_2 $E_{(1,0)}^{(\infty,xc)}$ takes into account a nonlocal part of the exchange-correlation interaction of electrons of d orbitals with the rest of the system. For WX_2 more delocalized electrons of the f orbitals contribute the value of $E_{(1,0)}^{(\infty,xc)}$. It is conceivable that the shift to more localized electrons corresponds to a more negative nonlocal part of the exchange-correlation energy ($-E_{(1,0)}^{(\infty,xc)}$ value), which is observed with the transition from W to Mo monolayer compounds.

The calculation of Kohn-Sham (KS) band gaps was performed for bulk and monolayer TMDs. For bulk materials using LDA (or PBE) we obtained the following KS band gaps 0.79 eV (0.93 eV) for MoS_2, 0.84 eV (0.81 eV) for $MoSe_2$, 0.98 eV (1.00 eV) for WS_2. The Kohn-Sham band gap obtained in LDA (or PBE) approximation for bulk TMD tend to underestimate the experimental band gap for about 0.31 eV (29%) for LDA and 0.35 eV (25%) for PBE GGA. Nevertheless for monolayers LDA (or PBE) KS band gaps of MoS_2 1.87 eV (1.62 eV), $MoSe_2$ 1.62 eV

Table 3. Theoretically obtained QP band gaps with GVJ-2e method (Eq. (3)), calculated GVJ-2e PL values, LDA2e band gaps (Eq. (2)), and correction terms Δ_{XC}^{∞} and $E_{(1,0)}^{(\infty,xc)}$ for bulk and monolayer MoS_2, $MoSe_2$, WS_2, WSe_2. Experimental values and theoretical band gaps obtained with other methods (GW, G_0W_0, HSE, TB-mBJ, sX) are referenced from the literature. All values are given in eV.

TMD	LDA_{2e}	Δ_{XC}^{∞}	$E_{(1,0)}^{(\infty,xc)}$	GW & G_0W_0	HSE	TB-mBJ	sX	GVJ-2e QP (GVJ-2e PL)	Exp.
MoS_2 Bulk	1.04	0.193	2.664	1.23[a]	1.46[e]	1.11[e]	1.35[g]	1.23	1.23[h]
				1.30[b]					
MoS_2 1L	2.33	−0.200	1.638	2.48[c]	2.02[d]	1.62[f]	1.88[g]	2.38 (PL 1.88)	1.89[i]
				2.97[b]					1.87, 1.9, 1.92[j]
									1.87[q]
$MoSe_2$ Bulk	1.17	−0.047	2.891	1.11[b), a]	1.36[e]	1.02[e]	1.16[g]	1.09	1.09[h]
$MoSe_2$ 1L	1.80	−0.134	1.636	2.18[c]	1.72[e]	1.40[f]	1.71[g]	2.03 (PL 1.57)	1.56[k]
				2.41[b]					1.55, 1.57, 1.58[l]
									1.52[q]
WS_2 Bulk	1.24	0.009	2.714	1.30[a]	1.60[e]	1.31[e]	1.44[g]	1.32	1.35[h]
WS2 1L	2.34	−0.190	−0.443	2.43[c]	1.98[d]	1.74[f]	2.13[g]	2.51 (PL 2.03)	2.01[m]
									1.98, 2.02, 2.05[n]
									1.99[q]
WSe_2 Bulk	1.23	−0.011	−0.541	1.19[a]	1.44[e]	1.20[e]	1.33[g]	1.21	1.20[h]
WSe_2 1L	1.90	−0.136	−0.221	2.08[c]	1.63[d]	1.43[f]	1.82[g]	2.11 (PL 1.67)	1.66[o]
									1.6, 1.64, 1.65[p]
									1.62[q]

[a] GW Ref. [35]; [b]GW Ref. [41]; [c]G0W0 Ref. [33]; [d]HSE for 1L TMDs Ref. [39]; [e]HSE and TB-mBJ for bulk TMDs Ref. [36]; [f]TB-mBJ for 1L TMDs Ref. [38]; [g]sX Ref. [40]; [h]Bulk TMDs experimental band gaps from Ref. [2]; [i]MoS_2 1L exp. Ref. [53]; [j]MoS_2 1L exp. Refs. [57–59]; [k]$MoSe_2$ 1L exp. Ref. [54]; [l]$MoSe_2$ 1L exp. Refs. [58,60,61]; [m]WS_2 1L exp. Ref. [55]; [n]WS_2 1L exp. Refs. [56,62,63]; [o]WSe_2 1L exp. Ref. [56]; [p]WSe_2 1L exp. Refs. [52,64,60]; [q]Our experimentally obtained band gaps.

(1.42 eV), WS_2 1.96 eV (1.73 eV), WSe_2 1.70 eV (1.51 eV) are much closer to the experimental values.

We calculated also the electronic band structures for bulk and monolayer TMDs. The bulk form of MoS_2, $MoSe_2$, WS_2, and WSe_2 are indirect band gap semiconductors with the valence band maximum (VBM) and conduction band minimum (CBM) located at G point and middle of K-G line in k-space, respectively. At the same time MoS_2, $MoSe_2$, WS_2 and WSe_2 monolayers are direct band semiconductors with both VBM and CBM located at K point (see **Figure 2)**). With transition from bulk to monolayer is observed transition from indirect to direct semiconductor. In Figure 2 the projected density of states (pDOS) is depicted. The density of states of the conduction band is formed largely by d states from metal atoms (Mo or W), which agree with published data.

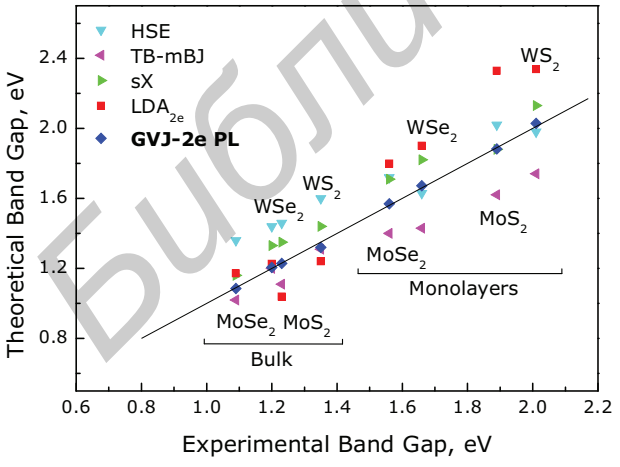

Figure 1. Comparison of the experimental PL and theoretical PL band gaps for bulk and monolayer TMDs. Theoretical PL band gaps include computed GVJ-2e and LDA_{2e}; HSE, TB-mBJ, sX values are taken from literature, see **Table 3**. As experimental band gap value is taken the first value from column Exp. PL in Table 3.

We have evaluated as well other well-accepted methods presented in Tables 2 and 3 and obtained the following results for MAE (and MAPD) on bulk and monolayer TMDs: GW 0.23 eV (10%), G_0W_0 0.09 eV (3%), HSE 0.17 eV (13%), TB-mBJ 0.14 eV (9%), sX 0.11 eV (8%) (see **Figure 3**). These results clearly demonstrate that the recently proposed method GVJ-2e implements a way to compute band gap values with much smaller average errors MAE 0.06 eV (2%) for GVJ-2e QP gaps and of 0.03 eV (2%) for PL band gaps. Although the precision of the GVJ-2e method overcomes the precision of hybrid functionals and GW methods, the GVJ-2e computational costs are comparable with one of LDA/GGA calculation. From Figure 3 follows that LDA_{2e} calculation could be also used for qualitative analysis of the fundamental band gap for new materials, as the accuracy of LDA_{2e} is comparable with accuracy of HSE method.

It is interesting to compare the behavior of the methods for the calculated band gap values for 3D (bulk) and 2D (monolayer) TMDs. GW and G_0W_0 methods tend to give a more accurate

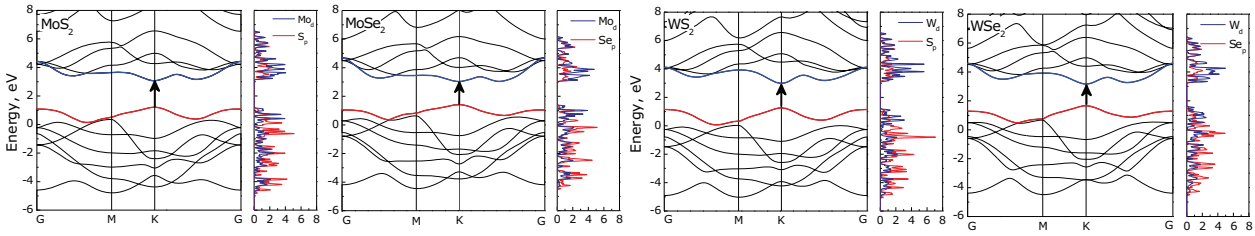

Figure 2. Theoretically obtained electronic band structures from LDA calculation (MoS_2 and $MoSe_2$) and from PBE calculation (WS_2 and WSe_2). The arrow indicates direct transition between VBM and CBM. On the right to the band structure, the projected density of states (pDOS [States/eV]) is plotted for each material (dark blue color corresponds to transition metal d states, red color corresponds to chalcogen p states).

band gap values for bulk TMDs, while larger errors occur for monolayers. The similar behavior is demonstrated by TB-mBJ functional, while opposite trend occurs for HSE which turns out to give better results for 2D structures. Proposed GVJ-2e method works equally well for both bulk and monolayer forms of TMDs.

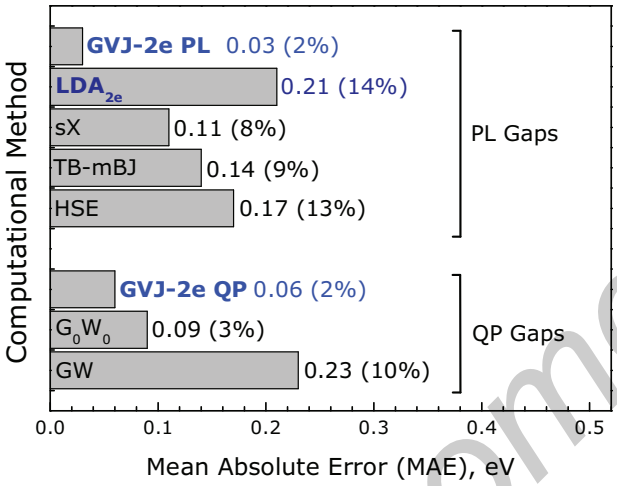

Figure 3. Calculated band gap mean absolute errors (MAE) for widely used methods (GW, G_0W_0, HSE, TB-mBJ, sX) and proposed GVJ-2e method for bulk and monolayer TMDs (band gap computed according to Eq. (3)). Also MAE for LDA_{2e} band gap is displayed (band gap computed according to Eq. (2)). Mean absolute percentage deviations (MAPD) are provided in %.

5. Conclusions

In this work, we have applied the general approach for the band gap calculations GVJ-2e (proposed by us earlier[45]) to analyze the electronic structure of the TMDs, which include the bulk form (3D representative with layered structure) and monolayer (2D structure). Similar to the case of conventional semiconductors and wide gap dielectrics, the calculated values of the band gap for bulk and monolayer TMDs are in very good agreement with the experimental values.

For bulk TMDs, the calculated band gaps are 1.23 eV (MoS_2), 1.09 eV ($MoSe_2$), 1.32 eV (WS_2), 1.21 eV (WSe_2). For monolayer TMDs, the calculated QP (and PL) band gaps are 2.38 eV (1.88 eV) for MoS_2, 2.03 eV (1.57 eV) for $MoSe_2$, 2.51 eV (2.03 eV) for WS_2, and 2.11 eV (1.67 eV) WSe_2. Although the precision of the GVJ-2e for TMD monolayers is close to one of G_0W_0 method, on both bulk and monolayer TMDs the GVJ-2e method has the smallest error of all. Thus the mean absolute error (MAE) of QP gaps for bulk and monolayer TMDs obtained with GVJ-2e method is 0.06 eV, which overcomes MAE of GW (0.23 eV) and G_0W_0 (0.09 eV) methods. For the GVJ-2e PL band gaps (calculated from GVJ-2e QP gaps) MAE is 0.03 eV, which is lower than MAE of other widely used methods such as HSE 0.17 eV, TB-mBJ 0.14 eV, and sX 0.11 eV. It should be mentioned that GVJ-2e method does not have inner limitations to a type of 2D system under investigation, thus could be potentially used for variety of other 2D materials (ex. AuPH[70]). We have demonstrated that, in agreement with the case of conventional semiconductors, the accuracy of the calculated band gaps is largely affected by the nonlocal part of the exchange-correlation energy. Accuracy and computational efficiency of the proposed GVJ-2e method enables using it for search and exploration of new materials (both 3D and 2D systems) with desired electronic properties.

Supporting Information

Supporting Information is available from the Wiley Online Library or from the author.

Acknowledgements

J. Gusakova, L. L. Shiau, X. Wang, and B. K. Tay gratefully acknowledge funding support from Ministry of Education, Singapore (Grant No.: MOE2015-T2-2-043).

Conflict of Interest

The authors declare no conflict of interest.

Keywords

band gap, density functional theory, electronic properties, layered materials, TMD

Received: April 11, 2017
Revised: September 5, 2017
Published online:

[1] K. S. Novoselov, D. Jiang, F. Schedin, T. J. Booth, V. V. Khotkevich, S. V. Morozov, A. K. Geim, *Proc. Nat. Acad. Sci. USA* **2005**, *102*, 10451.
[2] K. K. Kam, B. A. Parkinson, *J. Phys. Chem.* **1982**, *86*, 463.
[3] A. K. Geim, I. V. Grigorieva, *Nature* **2013**, *499*, 419.
[4] J.-W. Jiang, *Front. Phys.* **2015**, *10*, 106801.
[5] R. Lv, J. A. Robinson, R. E. Schaak, D. Sun, Y. Sun, T. E. Mallouk, M. Terrones, *Acc. Chem. Res.* **2015**, *48*, 56.
[6] M. Chhowalla, H. S. Shin, G. Eda, L.-J. Li, K. P. Loh, H. Zhang, *Nat. Chem.* **2013**, *5*, 263.
[7] K. Kalantar-Zadeh, J. Zh. Ou, T. Daeneke, M. S. Strano, M. Pumera, S. L. Gras, *Adv. Funct. Mater.* **2015**, *25*, 5086.
[8] B. Radisavljevic, A. Radenovic, J. Brivio, V. Giacometti, A. Kis, *Nat. Nanotechnol.* **2011**, *6*, 147.
[9] Y. Yoon, K. Ganapathi, S. Salahuddin, *Nano Lett.* **2011**, *11*, 3768.
[10] D. Kufer, G. Konstantatos, *Nano Lett.* **2015**, *15*, 7307.
[11] O. Lopez-Sanchez, D. Lembke, M. Kayci, A. Radenovic, A. Kis, *Nat. Nanotechnol.* **2013**, *8*, 497.
[12] Q. H. Wang, K. Kalantar-Zadeh, A. Kis, J. N. Coleman, M. S. Strano, *Nat. Nanotechnol.* **2012**, *7*, 699.
[13] A. Kuc, N. Zibouche, T. Heine, *Phys. Rev. B* **2011**, *83*, 245213.
[14] W. Kohn, *Rev. Mod. Phys.* **1999**, *71*, 1253.
[15] J. P. Perdew, A. Zunger, *Phys. Rev. B* **1981**, *23*, 5048.
[16] J. P. Perdew, Y. Wang, *Phys. Rev. B* **1986**, *33*, 8800(R).
[17] J. P. Perdew, Y. Wang, *Phys. Rev. B* **1992**, *45*, 13244.
[18] S. Kümmel, L. Kronik, *Rev. Mod. Phys.* **2008**, *80*, 3.
[19] J. Heyd, G. E. Scuseria, M. Ernzerhof, *J. Chem. Phys.* **2003**, *118*, 8207.
[20] J. Heyd, G. E. Scuseria, M. Ernzerhof, *J. Chem. Phys.* **2006**, *124*, 219906.
[21] J. Heyd, J. E. Peralta, G. E. Scuseria, R. L. Martin, *J. Chem. Phys.* **2005**, *123*, 174101.
[22] J. P. Perdew, M. Ernzerhof, *J. Chem. Phys.* **1996**, *105*, 9982.
[23] C. Lee, W. Yang, R. G. Parr, *Phys. Rev. B* **1988**, *37*, 785.
[24] A. D. Becke, *J. Chem. Phys.* **1993**, *98*, 1372.
[25] St. J. Clark, J. Robertson, *Phys. Rev. B* **2010**, *82*, 085208.
[26] N; Gidopoulos, S. Wilson, *The Fundamentals of Electron Density, Density Matrix and Density Functional Theory in Atoms, Molecules and the Solid State*, Springer Science + Business Media, Dordrecht **2003**, p. 145.
[27] Vl. I. Anisimov, J. Zaanen, O. K. Andersen, *Phys. Rev. B* **1991**, *44*, 943.
[28] A. I. Liechtenstein, V. I. Anisimov, J. Zaanen, *Phys. Rev. B* **1995**, *52*, R5467.
[29] A. D. Becke, E. R. Johnson, *J. Chem. Phys.* **2006**, *124*, 221101.
[30] F. Tran, P. Blaha, *Phys. Rev. Lett.* **2009**, *102*, 226401.
[31] L. Hedin, *Phys. Rev.* **1965**, *139*, A796.
[32] F. Aryasetiawan, O. Gunnarsson, *Rep. Prog. Phys.* **1998**, *61*, 237.
[33] F. A. Rasmussen, K. S. Thygesen, *J. Phys. Chem. C* **2015**, *119*, 13169.
[34] J. P. Perdew, K. Burke, M. Ernzerhof, *Phys. Rev. Lett.* **1996**, *77*, 3865.
[35] H. Jiang, *J. Phys. Chem. C* **2012**, *116*, 7664.
[36] W. Li, Ch. F. J. Walther, A. Kuc, T. Heine, *J. Chem. Theory Comput.* **2013**, *9*, 2950.
[37] S. Kumar, U. Schwingenschlögl, *Chem. Mater.* **2015**, *27*, 1278.
[38] N. Zibouche, A. Kuc, J. Musfeldt, T. Heine, *Ann. Phys.* **2014**, *526*, 395.
[39] J. Kang, S. Tongay, J. Zhou, J. Li, J. Wu, *Appl. Phys. Lett.* **2013**, *102*, 012111.
[40] Y. Guo, J. Robertson, *Appl. Phys. Lett.* **2016**, *108*, 233104.
[41] H.-P. Komsa, A. V. Krasheninnikov, *Phys. Rev. B* **2012**, *86*, 241201R.
[42] A. Molina-Sanchez, D. Sangalli, K. Hummer, A. Marini, L. Wirtz, *Phys. Rev. B* **2013**, *88*, 045412.
[43] T. Cheiwchanchamnangij, W. R. L. Lambrecht, *Phys. Rev. B* **2012**, *85*, 205302.
[44] J. Gusakova, B. K. Tay, V. Gusakov, Efficient DFT Method for Calculating Band Gap and Deep Levels in Semiconductors, 28th ICDS Conference, Helsinki, Finland (**2015**).
[45] J. Gusakova, B. K. Tay, V. Gusakov, *Phys. Status Solidi A* **2016**, *213*, 2834.
[46] Y. Gong, J. Lin, X. Wang, G. Shi, S. Lei, Z. Lin, X. Zou, G. Ye, R. Vajtai, B. I. Yakobson, H. Terrones, M. Ter-rones, Beng K. Tay, J. Lou, S. T. Pantelides, Z. Liu, W. Zhou, P. M. Ajayan, *Nat. Mater.* **2014**, *13*, 1135.
[47] X. Wang, Y. Gong, G. Shi, W. L. Chow, K. Keyshar, G. Ye, R. Vajtai, J. Lou, Z. Liu, E. Ringe, B. K. Tay, P. M. Ajayan, *ACS Nano* **2014**, *8*, 5125.
[48] H. Shi, L.-J. Li, Y. Li, *Chem. Soc. Rev.* **2015**, *44*, 2744.
[49] J. P. Perdew, M. Levy, *Phys. Rev. Lett.* **1983**, *51*, 1884.
[50] R. Coehoorn, C. Haas, J. Dijkstra, C. J. F. Flipse, R. A. Degroot, *Phys. Rev. B* **1987**, *35*, 6195.
[51] W. J. Schutte, J. L. De Boer, F. Jellinek, *J. Solid State Chem.* **1987**, *70*, 207.
[52] Y. Gong, G. Ye, S. Lei, G. Shi, Y. He, J. Lin, X. Zhang, R. Vajtai, S. T. Pantelides, W. Zhou, B. Li, P. M. Ajayan, *Adv. Funct. Mater.* **2016**, *26*, 2009.
[53] K. F. Mak, C. Lee, J. Hone, J. Shan, T. F. Heinz, *Phys. Rev. Lett.* **2010**, *105*, 136805.
[54] X. Lu, M. I. B. Utama, J. Lin, X. Gong, J. Zhang, Y. Zhao, S. T. Pantelides, J. Wang, Z. Dong, Z. Liu, W. Zhou, Q. Xiong, *Nano Lett.* **2014**, *14*, 2419.
[55] S. Tongay, W. Fan, J. Kang, J. Park, U. Koldemir, J. Suh, D. S. Narang, K. Liu, J. Ji, J. Li, R. Sinclair, J. Wu, *Nano Lett.* **2014**, *14*, 3185.
[56] W. Zhao, Z. Ghorannevis, L. Chu, M. Toh, C. Kloc, P.-H. Tan, G. Eda, *ACS Nano* **2013**, *7*, 791.
[57] J. O. Island, A. Kuc, E. H. Diependaal, R. Bratschitsch, H. S. J. van der Zant, T. Heine, A. Castellanos-Gomez, *Nanoscale* **2016**, *8*, 2589.
[58] S. Tongay, J. Zhou, C. Ataca, K. Lo, T. S. Matthews, J. Li, J. C. Grossman, J. Wu, *Nano Lett.* **2012**, *12*, 5576.
[59] Y. L. Huang, Y. Chen, W. Zhang, S. Y. Quek, C.-H. Chen, L.-J. Li, W.-T. Hsu, W.-H. Chang, Y. J. Zheng, W. Chen, A. T. S. Wee, *Nat. Commun.* **2015**, *6*, 6298.
[60] P. Tonndorf, R. Schmidt, P. Böttger, X. Zhang, J. Börner, A. Liebig, M. Albrecht, C. Kloc, O. Gordan, D. R. T. Zahn, S. M. de Vasconcellos, R. Bratschitsch, *Opt. Express* **2013**, *21*, 4908.
[61] Y. Zhang, T.-R. Chang, B. Zhou, Y.-T. Cui, H. Yan, Z. Liu, F. Schmitt, J. Lee, R. Moore, Y. Chen, H. Lin, H.-T. Jeng, S.-K. Mo, Z. Hussain, A. Bansil, Z.-X. Shen, *Nat. Nanotechnol.* **2014**, *9*, 111.
[62] A. L. Elias, N. Perea-Lopez, A. Castro-Beltran, A. Berk-demir, R. Lv, S. Feng, A. D. Long, T. Hayashi, Y. A. Kim, M. Endo, H. R. Gutierrez, N. R. Pradhan, L. Balicas, T. E. Mallouk, F. Lopez-Urias, H. Terrones, M. Terro-nes, *ACS Nano* **2013**, *7*, 5235.
[63] H. R. Gutierrez, N. Perea-Lopez, A. L. Elias, A. Berkdemir, B. Wang, R. Lv, F. Lopez-Urias, V. H. Crespi, H. Terrones, M. Terrones, *Nano Lett.* **2013**, *13*, 3447.
[64] B. W. H. Baugher, H. O. H. Churchill, Y. Yang, P. Jarillo-Herrero, *Nat. Nanotechnol.* **2014**, *9*, 262.
[65] T. Olsen, S. Latini, F. Rasmussen, K. S. Thygesen, *PRL* **2016**, *116*, 056401.
[66] A. R. Klots, A. K. M. Newaz, Bin Wang, D. Prasai, H. Krzyzanowska, J. Lin, D. Caudel, N. J. Ghimire, J. Yan, B. L. Ivanov, K. A. Velizhanin, A. Burger, D. G. Mandrus, N. H. Tolk, S. T. Pantelides, K. I. Bolotin, *Sci. Rep.* **2014**, *4*, 6608.
[67] M. M. Ugeda, A. J. Bradley, S.-F. Shi, F. H. da Jornada, Y. Zhang, D. Y. Qiu, W. Ruan, S.-K. Mo, Z. Hussain, Z.-X. Shen, F. Wang, S. G. Louie, M. F. Crommie, *Nat. Mater.* **2014**, *13*, 1091.
[68] B. Zhu, X. Chen, X. Cui, *Sci. Rep.* **2015**, *5*, 1.
[69] C. Zhang, Y. Chen, A. Johnson, M.-Y. Li, L.-J. Li, P. C. Mende, R. M. Feenstra, C.-K. Shih, *Nano Lett.* **2015**, *15*, 6494.
[70] L. Tsetseris, *FlatChem* **2017**, *2*, 49.